Connectivity of Multiple Cooperative Cognitive Radio Ad Hoc Networks

Weng Chon Ao, Shin-Ming Cheng, *Member, IEEE,* and Kwang-Cheng Chen, *Fellow, IEEE*

***Abstract*—In cognitive radio networks, the signal reception quality of a secondary user degrades due to the interference from multiple heterogeneous primary networks, and also the transmission activity of a secondary user is constrained by its interference to the primary networks. It is difficult to ensure the connectivity of the secondary network. However, since there may exist multiple heterogeneous secondary networks with different radio access technologies, such secondary networks may be treated as one secondary network via proper cooperation, to improve connectivity. In this paper, we investigate the connectivity of such a cooperative secondary network from a percolation-based perspective, in which each secondary network's user may have other secondary networks' users acting as relays. The connectivity of this cooperative secondary network is characterized in terms of percolation threshold, from which the benefit of cooperation is justified. For example, while a noncooperative secondary network does not percolate, percolation may occur in the cooperative secondary network; or when a noncooperative secondary network percolates, less power would be required to sustain the same level of connectivity in the cooperative secondary network.**

***Index Terms*—cognitive radio networks, connectivity, cooperation, heterogeneous wireless networks, ad hoc networks**

I. INTRODUCTION

COGNITIVE radio networking has emerged as a promising technology to enhance spectrum utilization by sensing the spectrum and opportunistically accessing the spectrum of primary (licensed) systems [1], [2]. The spectrum sharing model can be practically divided into two main approaches: *interweave* and *underlay* [3]. In the interweave approach, secondary (unlicensed) users (SUs) embedded with cognitive radios orthogonally access temporary spectrum holes of primary systems facilitated by the advanced spectrum sensing and signal processing techniques. In the underlay approach, primary users (PUs) and SUs transmit at the same time while SUs are considered of lower priority in spectrum access. Their interference to PUs should be limited by an interference temperature [4] indicating the maximum tolerable interference power. This paper focuses on the underlay approach. It is important to understand the connectivity of the secondary network so that proper network operations can be performed. However, different from a homogeneous network user, the signal reception quality of an SU further degrades due to the inter-system interference from PUs, and also the transmission activity of an SU is constrained by its interference to PUs. It is much harder to ensure the connectivity of the secondary network. As a result, if multiple secondary networks can cooperate with each other by having other secondary networks' nodes acting as relays, connectivity may be improved[1].

Connectivity of a homogeneous wireless ad hoc network has been widely studied in different aspects. In [5], n nodes are uniformly distributed in a unit square where two nodes are connected if their distance is smaller than $r(n)$. To ensure 1-connectivity of the network, i.e., a path exists between any pair of nodes, $r(n) = \sqrt{\frac{\log n + c(n)}{\pi n}}$ where $c(n) \to \infty$ as $n \to \infty$. In [6], k-connectivity of a network, i.e., at least k node-disjoint paths exist between any pair of nodes, was studied. On the other hand, in many applications such as sensor networks and mobile ad hoc networks, 1-connectivity is not required. A weaker connectivity from a percolation-based perspective (i.e., a nonvanishing fraction of nodes in the network, say, 95%, are connected) is more suitable, for example, significant savings in power consumption can be achieved by allowing a small fraction (say, 5%) of nodes to be disconnected [7], [8]. For an infinite network with density λ and transmission range r (i.e., a random geometric network), the network percolates in which an infinite connected component appears when the average degree of a network node is above a certain number (i.e., $\lambda \pi r^2 \geq 4.52$ [9]). Otherwise, the network does not percolate and consists of many isolated finite clusters. In our study, a secondary user may be deactivated or disconnected from each other due to the appearance of primary transmissions so that 1-connectivity in the secondary network may not be feasible, justifying investigation of connectivity of secondary network from a percolation-based approach.

In [10], [11], the effect of fading on the mean degree of a network node was discussed. In [7], [12], the impact of fading on the percolation of a wireless ad hoc network was investigated. The effect of self co-channel interference was considered in [13] and the authors proposed a Signal To Interference Ratio Graph (STIRG) to study percolation in ad hoc network. Connectivity of a network with unreliable links was studied in [14] in a percolation sense. Percolation of a cooperative wireless ad hoc network was addressed in [15], in which nodes may form a group to perform distributed beamforming so that signals are coherently combined at some destinations. Long range transmissions can be established and thus connectivity is improved. Note that all the above works were focused on connectivity of a homogeneous ad hoc

Manuscript received 14 February 2011; revised 14 July 2011. This research is sponsored by the National Science Council under the contract of NSC 98-2221-E-002-065-MY3, NSC 99-2911-I-002-001, and NSC 99-2911-I-002-201.

W. C. Ao, S.-M. Cheng, and K.-C. Chen are with the Graduate Institute of Communication Engineering, National Taiwan University, Taipei, Taiwan (e-mail: r97942044@ntu.edu.tw, smcheng@cc.ee.ntu.edu.tw, and chenkc@cc.ee.ntu.edu.tw).

Digital Object Identifier 10.1109/JSAC.2012.120204.

[1]Note that in this paper multiple secondary networks cooperate with each other by relaying (carrying) each other's traffic, which is different from physical layer cooperative techniques such as distributed beamforming.

network. Connectivity of heterogeneous wireless networks, specifically cognitive radio networks, has been recently investigated in [16]–[18]. In [16], the connectivity of a secondary network is parameterized by the tuple $(\lambda_{PT}, \lambda_{SU})$ under path loss channel model, where λ_{PT} is the density of primary transmitters and λ_{SU} is the density of SUs. Percolation of the secondary network occurs only when λ_{PT} is below some threshold and λ_{SU} is above some threshold. Another parameterization of the secondary network (λ_{SU}, r_{SU}) is developed in [17] under Rayleigh fading channel model, where r_{SU} is the transmission range of an SU with an outage constraint. The temporal activity of a spectrum opportunity is further captured in [18]. In spite of the above efforts, the connectivity of cooperative secondary network has not been investigated.

In this paper, we therefore analyze the benefit of cooperation among multiple secondary networks from a percolation-based perspective. Quantification of connectivity improvement with network-based cooperation facilitates network control and design. To our knowledge, it is the first framework to jointly consider the effects of cooperation (among multiple secondary networks), interference (from multiple primary networks), heterogeneity (in different priorities of spectrum access), and general fading on the percolation of wireless networks. Our framework can be summarized into four steps. In the first step, we derive the degree distribution of an SU in a secondary ad hoc network[2] sustaining interference from multiple heterogeneous primary ad hoc networks under general fading of desired signal and interfering signals. The relationship between the degree distribution of a wireless network node and the connectivity of the wireless network in percolation sense can be established by extending the methods of complex networks [19], [20]. In the second step, we obtain the active probability of an SU. An SU can transmit (or be active) only when its interference power to each primary receiver in primary networks is below the interference temperature. In the third step, with both the degree distribution and the active probability of an SU, percolation threshold of a single secondary network is derived by using the site-percolation model [21]. The site-percolation model is widely used to study percolation of a network (of some degree distribution) with random node failures. A random node failure is analogous to the deactivation of an SU in our study. In the fourth step, we investigate the connectivity of cooperative secondary network in which each secondary network's node may have other secondary networks' nodes acting as relays. The benefit of cooperation among multiple heterogeneous secondary networks is analytically characterized in terms of percolation threshold.

The remainder of this paper is organized as follows. Section II provides background on degree distribution of a stand-alone wireless fading network and percolation analysis. In Section III, we present the network model, the degree distribution of an SU, the active probability of an SU, the mapping to site-percolation model, and the optimal power allocation among SUs. In Section IV, we study percolation in cooperative secondary network. Numerical results are provided in Section V. Section VI gives the conclusion.

[2]In an ad hoc network, the nodes are distributed as a homogeneous Poisson point process, and two nodes are connected by a link if the channel between them can support a given information rate.

II. Background

A. Degree distribution of a stand-alone wireless network

We consider a stand-alone wireless ad hoc network, in which the spatial distribution of nodes is assumed to follow a homogeneous Poisson point process (PPP) with density λ. Let $\Phi = \{X_k\}$ denote the set of locations of the nodes and let P denote the transmit power of a node. A pair of nodes are connected if the capacity of the channel between them can support an information rate R, which happens when $\log\left(1 + \frac{G_X P r^{-\alpha}}{N_0}\right) \geq R$, where G_X denotes the channel power gain, r is the distance between the pair of nodes, α is the path loss exponent, and N_0 is the background noise power.

Consequently, neighbors of a typical node (a reference node located at the origin)[3] are resulted from independently thinning of each node $X_k \in \Phi$ with probability $\mathbb{P}\left(G_{X_k} \geq \frac{(2^R-1)N_0}{P\|X_k\|^{-\alpha}}\right)$. G_{X_k} denotes the channel power gain of the desired link from the typical node to the node at X_k, which is independently drawn according to some distribution f_{G_X}, i.e., the distribution function $f_{G_{X_k}}(x) = f_{G_X}(x),\ \forall k$. $\|X_k\|$ denotes the distance between the typical node and the node at X_k. By the mapping theorem [11], [22], the number of neighbors (or the degree) of the typical node is Poisson distributed with mean β

$$\beta = \int_0^\infty \lambda \mathbb{P}\left(G_X \geq \frac{(2^R-1)N_0}{Pr^{-\alpha}}\right) 2\pi r dr$$
$$= \lambda\pi \left(\frac{(2^R-1)N_0}{P}\right)^{-\delta} \mathbb{E}[G_X^\delta], \tag{1}$$

where $\delta = \frac{2}{\alpha}$. The probability that a node has k neighbors is denoted as p_k, which satisfies

$$p_k = \frac{\exp(-\beta)\beta^k}{k!},\ k = 0, 1, 2, \dots \tag{2}$$

The probability that a node has no neighbors (or the node isolation probability) is $\exp(-\beta)$. Note that in the case without fading, the average number of neighbors of a node (or the mean degree) is $\lambda\pi\left(\frac{(2^R-1)N_0}{P}\right)^{-\delta}$, implying that $\mathbb{E}[G_X^\delta]$ corresponds to the *connectivity fading gain* [10], [11].

B. Percolation analysis

The concept of percolation is originated from statistical physics and random networks [9], [20]. In our study, as the transmit power of a node P increases, the mean degree β increases. If we draw links between each node and its neighbors, the resulting network graph percolates (i.e., an infinite connected component appears in the network) when β is above a percolation threshold β_{th}. On the other hand, when β is below the percolation threshold, the network does not percolate and consists of many isolated finite components. The percolation threshold β_{th} can be computed by finding the critical point at which the mean component size blows up, indicating the formation of an infinite connected component.

[3]By the stationary characteristic of homogeneous PPP [22], the statistics measured by the typical node is representative for all other nodes. Therefore, we focus our discussions on the typical node. A typical node may be a transmitter or a receiver depending on the context.

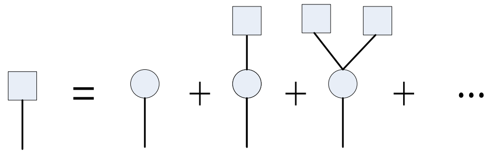

Fig. 1. An illustration of the self-consistency relation $H_1(x) = x\sum_{k=0}^{\infty} q_k(H_1(x))^k = xF_1(H_1(x))$. A square represents the connected component of nodes reached by following a randomly selected link, and a circle represents the node first reached. The component size can be expressed as the sum of the probabilities of having only a single node, having a single node connected to one other component, etc.

We describe the procedure of finding the percolation threshold as follows.

We first define the generating function of the degree distribution of a randomly selected node as $F_0(x) = \sum_{k=0}^{\infty} p_k x^k = \exp(\beta(x-1))$. Also, we define the excess degree[4] distribution of a node at the end of a randomly selected link as q_k. Since it is more likely to arrive at a node that has a higher degree by following a randomly selected link, $q_k = (k+1)p_{k+1}/\sum_k kp_k = (k+1)p_{k+1}/\beta$ is proportional to kp_k [23]. The generating function of q_k is defined as $F_1(x) = \sum_{k=0}^{\infty} q_k x^k$, and we can easily verify that $F_1(x) = F_0'(x)/\beta = \exp(\beta(x-1))$, where $F_0'(x)$ denotes the derivative of $F_0(x)$. Moreover, the generating function of the total number of nodes reachable by following a randomly selected link (resp. node) is defined as $H_1(x)$ (resp. $H_0(x)$), which satisfies the self-consistency relation $H_1(x) = x\sum_{k=0}^{\infty} q_k(H_1(x))^k = xF_1(H_1(x))$ (resp. $H_0(x) = x\sum_{k=0}^{\infty} p_k(H_1(x))^k = xF_0(H_1(x))$). An illustration is provided in Fig. 1. Consequently, the average total number of nodes (or the mean component size) reachable from a randomly selected node is $H_0'(1) = 1 + \frac{F_0'(1)}{1-F_1'(1)}$, which blows up when $1 - F_1'(1) = 0$ indicating the formation of an infinite connected component. Here in the Poisson case, it corresponds to $1-\beta = 0$, and the percolation threshold $\beta_{th} = 1$ is obtained. More details can be found in [20], [23], [24].

Note that the above formulation ignores the spatial dependency (i.e., two of a node's neighbors are likely neighbors themselves). The actual percolation threshold is offset with a small constant depending on the fading distribution. In the case without fading, the network graph is the so-called random geometric graph with $\beta_{th} \approx 4.52$, while channel fading produces spread-out connections and weakens the spatial dependency, and thus reduces the percolation threshold [7], [12], [25]. In our analysis, the spatial dependency may be further reduced due to the randomness from the interference, and we justify that the spatial dependency is small before the secondary network percolates in Appendix A of [26]. In Section IV of the paper, we follow the approach in [20], [23], [24] to provide benchmark comparison of the percolation thresholds of a noncooperative secondary network and the cooperative one.

III. Network Model and Analytic Methods

We consider a secondary network (denoted as SN_0), in which the spatial distribution of SUs is assumed to follow a

[4]Excess degree of a node is one less than its total degree.

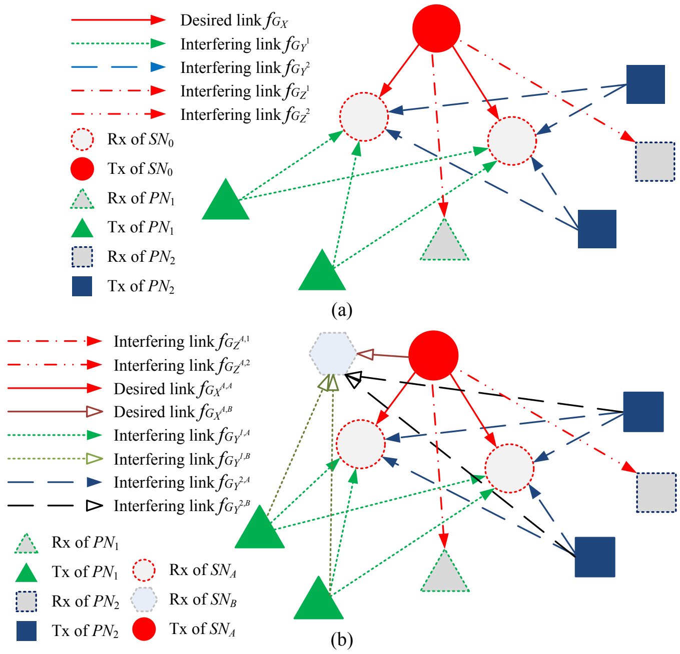

Fig. 2. (a) A transmitter (Tx) in SN_0 broadcasts a message while receivers (Rx) in SN_0 sustain interference from heterogeneous primary networks PN_1 and PN_2. The channel power gain of the desired link is drawn according to distribution f_{G_X}, the channel power gain of the interfering link from PN_1 (PN_2) to SN_0 is drawn according to distribution $f_{G_{Y^1}}$ ($f_{G_{Y^2}}$), and the channel power gain of the interfering link from SN_0 to PN_1 (PN_2) is drawn according to distribution $f_{G_{Z^1}}$ ($f_{G_{Z^2}}$). (b) A cooperative secondary network consisting of SN_A and SN_B sustains interference from heterogeneous primary networks PN_1 and PN_2.

PPP with density λ. Let $\Phi = \{X_k\}$ denote the set of locations of the SUs and let P denote the transmit power of an SU. SN_0 coexists with N heterogeneous primary networks (denoted as PN_i, $1 \le i \le N$), where the spatial distribution of PTs (resp. PRs) in PN_i is assumed to follow a PPP with density μ_i^{PT} (resp. μ_i^{PR}).[5] The set of locations of the PTs in PN_i is denoted as $\Psi_i^{PT} = \{Y_k^i\}$ and the transmit power of a PT in PN_i is P_i. The set of locations of the PRs in PN_i is denoted as $\Psi_i^{PR} = \{Z_k^i\}$ and the interference temperature at a PR in PN_i is τ_i. The interference from the PTs in PN_i to a typical SU of SN_0 is denoted as $I_i = \sum_{Y_k^i \in \Psi_i^{PT}} G_{Y_k^i} P_i \|Y_k^i\|^{-\alpha}$. $G_{Y_k^i}$ denotes the channel power gain of the interfering link from the PT at Y_k^i to the typical SU, which is assumed to be independently drawn from $f_{G_{Y^i}}$, i.e., the distribution function $f_{G_{Y_k^i}}(x) = f_{G_{Y^i}}(x)$, $\forall k$. $\|Y_k^i\|$ is the distance between the PT at Y_k^i and the typical SU, and α is the path loss exponent. All packet transmissions of the networks are assumed to be slotted and synchronized. Since SN_0 operates in an interference-limited environment, we ignore the background noise.

As a result, neighbors of a typical SU of SN_0 are resulted from independently[6] thinning of each SU $X_k \in \Phi$ with probability $\mathbb{P}\left(\log\left(1 + \frac{G_{X_k} P \|X_k\|^{-\alpha}}{\sum_{i=1}^{N} I_i}\right) \ge R\right)$, where G_{X_k} de-

[5]For example, in PN_i, each PT has a dedicated PR at distance d away with an arbitrary direction so that the PRs also form a PPP with density $\mu_i^{PR} = \mu_i^{PT}$.

[6]We assume that the spatial correlation of interference observed at different nodes in Φ can be ignored due to the i.i.d. channel gains in different pairs of nodes [27]. This assumption leads to the Poisson degree distribution of an SU. Theorem III.1-III.3 (about the mean $\widetilde{\beta}$) still hold without this assumption.

notes the channel power gain of the desired link from the typical SU to the SU at X_k, which is assumed to be independently drawn from f_{G_X}, i.e., the distribution function $f_{G_{X_k}}(x) = f_{G_X}(x),\ \forall k$. $\|X_k\|$ denotes the distance between the typical SU and the SU at X_k, and R denotes the information rate. An illustration of above scenario is provided in Fig. 2(a). By the mapping theorem, the number of neighbors of a typical SU of SN_0 is Poisson distributed with mean $\widetilde{\beta} = \int_0^\infty \lambda \mathbb{P}\left(G_X \geq \frac{(2^R-1)(\sum_{i=1}^N I_i)}{Pr^{-\alpha}}\right) 2\pi r dr$, which is further computed in the next subsection.

A. Degree distribution of an SU

Theorem III.1. *Under general fading of both desired signal and interfering signals, $\widetilde{\beta}$ is bounded above by*

$$\widetilde{\beta} < \frac{\lambda P^\delta \mathbb{E}[G_X^\delta]}{\left(\sum_{i=1}^N \mu_i^{PT} P_i^\delta \mathbb{E}[G_{Y^i}^\delta]\right)(2^R-1)^\delta} \triangleq \widetilde{\beta}^{Upper}, \quad (3)$$

where $\delta = \frac{2}{\alpha}$.

Proof: The proof is presented in Appendix B of [26]. ∎

Theorem III.2. *Under general fading of both desired signal and interfering signals, $\widetilde{\beta}$ is computed in nearly closed form*

$$\widetilde{\beta} = \frac{\lambda P^\delta \int_{-\infty}^\infty \frac{g(t)}{t^\delta} dt}{\left(\sum_{i=1}^N \mu_i^{PT} P_i^\delta \mathbb{E}[G_{Y^i}^\delta]\right)(2^R-1)^\delta \Gamma(1-\delta)}. \quad (4)$$

$g(t)$ is the inverse Laplace transform of $\overline{F}_{G_X}(s)$ satisfying $\overline{F}_{G_X}(s) = \mathcal{L}\{g(t)\} = \int_{-\infty}^\infty e^{-st} g(t) dt$, where $\overline{F}_{G_X}(s) = \mathbb{P}(G_X \geq s)$ is the ccdf (complementary cumulative distribution function) of the channel power gain of the desired link. $\Gamma(z) = \int_0^\infty t^{z-1} e^{-t} dt$ is the Gamma function.

Proof: The proof is presented in Appendix C of [26]. ∎

For example, when the desired link is Rayleigh faded, i.e., the channel power gain G_X is exponentially distributed (with unit mean, without loss of generality), we have $\overline{F}_{G_X}(s) = e^{-s} = \mathcal{L}\{\delta(t-1)\}$ where $\delta(t)$ is the Dirac delta function. We can thus compute the expression $\int_{-\infty}^\infty \frac{g(t)}{t^\delta} dt = \int_{-\infty}^\infty \frac{\delta(t-1)}{t^\delta} dt = 1$ and obtain $\widetilde{\beta} = \frac{\lambda P^\delta}{\left(\sum_{i=1}^N \mu_i^{PT} P_i^\delta \mathbb{E}[G_{Y^i}^\delta]\right)(2^R-1)^\delta \Gamma(1-\delta)}$.

Theorem III.3. *Under general fading of both desired signal and interfering signals, $\widetilde{\beta}$ is bounded below by*

$$\widetilde{\beta} \geq \frac{\lambda P^\delta \mathbb{E}[G_X^\delta](1-\frac{2}{\alpha-2})^+}{\left(\sum_{i=1}^N \mu_i^{PT} P_i^\delta \mathbb{E}[G_{Y^i}^\delta]\right)(2^R-1)^\delta} \triangleq \widetilde{\beta}^{Lower}, \quad (5)$$

where $(x)^+ \triangleq \max(x, 0)$. The lower bound is non-trivial when $\alpha > 4$.

Proof: The proof is presented in Appendix D of [26]. ∎

We compare $\widetilde{\beta}^{\text{Upper}}$ with $\widetilde{\beta}^{\text{Lower}}$, it is observed that

$$\frac{\widetilde{\beta}^{\text{Upper}}}{\widetilde{\beta}^{\text{Lower}}} = \frac{1}{(1-\frac{2}{\alpha-2})^+}. \quad (6)$$

The ratio between the upper bound and the lower bound is a constant depending on the path loss exponent. Note that when $\alpha \to \infty$, $\widetilde{\beta}^{\text{Upper}}/\widetilde{\beta}^{\text{Lower}} \to 1$ (i.e., the bounds are asymptotically tight), suggesting that outage is mainly caused by dominating interferers [26] as the path loss exponent is large.

We conclude that the degree distribution of an SU sustaining interference from multiple heterogeneous primary networks (denoted as $\tilde{p}_k$) is a Poisson distribution with mean $\widetilde{\beta}$, i.e.,

$$\tilde{p}_k = \frac{\exp(-\widetilde{\beta})\widetilde{\beta}^k}{k!},\ k = 0, 1, 2, \ldots \quad (7)$$

B. Active probability of an SU

The interference power from a typical SU of SN_0 to the PR at $Z_k^i \in \Psi_i^{PR}$ is $G_{Z_k^i} P \|Z_k^i\|^{-\alpha}$, where $G_{Z_k^i}$ denotes the channel power gain of the interfering link from the typical SU to the PR at Z_k^i, which is assumed to be independently drawn from $f_{G_{Z^i}}$, i.e., the distribution function $f_{G_{Z_k^i}}(x) = f_{G_{Z^i}}(x),\ \forall k$. $\|Z_k^i\|$ denotes the distance between the typical SU and the PR at Z_k^i. An illustration is provided in Fig. 2(a). We define the set $\Xi_i^{PR} = \{Z_k^i \in \Psi_i^{PR} : G_{Z_k^i} P \|Z_k^i\|^{-\alpha} > \tau_i\}$. Ξ_i^{PR} consists of PRs in PN_i whose received interference power from the typical SU exceeds the interference temperature τ_i.

From mapping theorem, the number of PRs in Ξ_i^{PR} is Poisson distributed with mean ν_i

$$\begin{aligned}
\nu_i &= \int_0^\infty \mu_i^{PR} \mathbb{P}\left(G_{Z^i} P r^{-\alpha} > \tau_i\right) 2\pi r dr \\
&= \mathbb{E}_{G_{Z^i}}\left[\int_0^\infty \mu_i^{PR} \mathbf{1}\left(r < (G_{Z^i} P \tau_i^{-1})^{\frac{1}{\alpha}}\right) 2\pi r dr\right] \\
&= \mathbb{E}_{G_{Z^i}}\left[\mu_i^{PR} \pi (G_{Z^i} P \tau_i^{-1})^\delta\right] \\
&= \mu_i^{PR} \pi P^\delta \mathbb{E}[G_{Z^i}^\delta] \tau_i^{-\delta}, \quad (8)
\end{aligned}$$

where $\mathbf{1}(\cdot)$ is the indicator function. An SU can be active only when there are no PRs in $\Xi_i^{PR},\ \forall i,\ 1 \leq i \leq N$. Thus, the active probability of an SU (denoted as p^a) can be computed as

$$\begin{aligned}
p^a &= \prod_{i=1}^N \mathbb{P}(\Xi_i^{PR} = \phi) \\
&= \prod_{i=1}^N \exp(-\nu_i) \\
&\overset{(a)}{=} \prod_{i=1}^N \exp\left(-\mu_i^{PR} \pi P^\delta \mathbb{E}[G_{Z^i}^\delta] \tau_i^{-\delta}\right) \\
&= \exp\left(-\left(\sum_{i=1}^N \mu_i^{PR} \mathbb{E}[G_{Z^i}^\delta] \tau_i^{-\delta}\right) \pi P^\delta\right), \quad (9)
\end{aligned}$$

where (a) follows (8).

C. Mapping to site-percolation model

From Section III-A and Section III-B, we obtain the degree distribution of an SU (i.e., $\tilde{p}_k$), which is Poisson with mean $\widetilde{\beta}$, and the active probability of an SU p^a. Now, we are able to derive the percolation threshold of the secondary network SN_0 by extending the analysis in Section II-B to the scenario with random node failure (deactivation of an SU) with probability $1 - p^a$, using the site percolation model [21].

We define the generating function of the degree distribution of a randomly selected SU as $\widetilde{F}_0(x) = \sum_{k=0}^{\infty} \tilde{p}_k x^k = \exp(\widetilde{\beta}(x-1))$. The excess degree distribution of an SU at the end of a randomly selected link is defined as $\tilde{q}_k$, which satisfies $\tilde{q}_k = (k+1)\tilde{p}_{k+1}/\sum_k k\tilde{p}_k = (k+1)\tilde{p}_{k+1}/\widetilde{\beta}$. The generating function of $\tilde{q}_k$ is defined as $\widetilde{F}_1(x) = \sum_{k=0}^{\infty} \tilde{q}_k x^k$, and we can easily verify that $\widetilde{F}_1(x) = \widetilde{F}_0'(x)/\widetilde{\beta} = \exp(\widetilde{\beta}(x-1))$. Moreover, the generating function of the total number of active SUs reachable by following a randomly selected link (resp. SU) is defined as $\widetilde{H}_1(x)$ (resp. $\widetilde{H}_0(x)$), which satisfies the self-consistency relation $\widetilde{H}_1(x) = 1 - p^a + p^a x \sum_{k=0}^{\infty} \tilde{q}_k (\widetilde{H}_1(x))^k = 1 - p^a + p^a x \widetilde{F}_1(\widetilde{H}_1(x))$ (resp. $\widetilde{H}_0(x) = 1 - p^a + p^a x \sum_{k=0}^{\infty} \tilde{p}_k (\widetilde{H}_1(x))^k = 1 - p^a + p^a x \widetilde{F}_0(\widetilde{H}_1(x))$). Consequently, the average total number of active SUs reachable from a randomly selected SU (or the mean size of a cluster of connected and active SUs) is $\widetilde{H}_0'(1) = p^a \left[1 + p^a \widetilde{F}_0'(1)/(1 - p^a \widetilde{F}_1'(1))\right]$, which blows up when $1 - p^a \widetilde{F}_1'(1) = 0$ indicating the formation of an infinite connected component. Here in the Poisson case, it corresponds to $1 - p^a \widetilde{\beta} = 0$ and we obtain the percolation threshold $\widetilde{\beta}_{th} = 1/p^a$.

D. Optimal power allocation

We observe that when an SU's transmit power P decreases, its active probability increases; however, its mean degree $\widetilde{\beta}$ decreases. We maximize the effective mean degree of an SU with respect to P, which is defined as the product of its active probability and its mean degree. That is,

$$p^a \widetilde{\beta} = \exp\left(-\left(\sum_{i=1}^{N} \mu_i^{PR} \mathbb{E}[G_{Z^i}^\delta] \tau_i^{-\delta}\right) \pi P^\delta\right) \times \frac{\lambda P^\delta \mathbb{E}[G_X^\delta]}{\left(\sum_{i=1}^{N} \mu_i^{PT} P_i^\delta \mathbb{E}[G_{Y^i}^\delta]\right)(2^R - 1)^\delta}. \quad (10)$$

Note that we use the upper bound on $\widetilde{\beta}$ in Theorem III.1. After some calculations, the optimal transmit power is $P^* = \left(\pi \sum_{i=1}^{N} \mu_i^{PR} \mathbb{E}[G_{Z^i}^\delta] \tau_i^{-\delta}\right)^{-\delta^{-1}}$, which maximizes the effective mean degree of an SU.

IV. Cooperation among heterogeneous secondary networks

As discussed in Section III-C, when the mean degree of a secondary network node is lower than the percolation threshold $\widetilde{\beta}_{th}$, the secondary network does not percolate. We here propose and prove that different secondary networks may cooperate with each other by having other secondary networks' nodes acting as relays to improve network connectivity. The benefit of cooperation among heterogeneous secondary networks can be quantified in terms of percolation threshold. We first focus on the case with cooperation between two heterogeneous secondary networks coexisting with N heterogeneous primary networks. Then, the result is extended to the case with cooperation among multiple heterogeneous secondary networks.

Suppose that there are two secondary networks (denoted as SN_A and SN_B), respectively with node density λ_A and λ_B, with set of locations of nodes $\Phi_A = \{X_k^A\}$ and $\Phi_B = \{X_k^B\}$, with transmit power P_A and P_B, and with information rate R_A and R_B. The channel power gain of the link between a transmitting node in $SN_u,\ u \in \{A, B\}$ and a receiving node in $SN_v,\ v \in \{A, B\}$ is assumed to be drawn according to some distribution $f_{G_{X^{u,v}}}$. Furthermore, the channel power gain of the interfering link from a PT in $PN_i,\ 1 \le i \le N$ to a receiving node in $SN_v,\ v \in \{A, B\}$ is assumed to be drawn according to some distribution $f_{G_{Y^{i,v}}}$. An illustration is provided in Fig. 2(b). The average number of neighbors in $SN_v,\ v \in \{A, B\}$ of a node of $SN_u,\ u \in \{A, B\}$ is denoted as $\widetilde{\beta}_{u,v}$.

We take $\widetilde{\beta}_{A,B}$ as an example. With cooperation, a node in SN_B listens the message from a node of SN_A, and decoding succeeds with probability

$$\mathbb{P}\left(\log\left(1 + \frac{G_{X^{A,B}} P_A r^{-\alpha}}{\sum_{i=1}^{N} I_i}\right) \ge R_A\right), \quad (11)$$

where r is the distance between the pair of nodes. By using Theorem III.1, the number of neighbors in SN_B of a node of SN_A is Poisson distributed with mean $\widetilde{\beta}_{A,B}$, where

$$\widetilde{\beta}_{A,B} = \int_0^\infty \lambda_B \mathbb{P}\left(G_{X^{A,B}} \ge \frac{(2^{R_A} - 1)(\sum_{i=1}^{N} I_i)}{P_A r^{-\alpha}}\right) 2\pi r dr < \frac{\lambda_B P_A^\delta \mathbb{E}[G_{X^{A,B}}^\delta]}{\left(\sum_{i=1}^{N} \mu_i^{PT} P_i^\delta \mathbb{E}[G_{Y^{i,B}}^\delta]\right)(2^{R_A} - 1)^\delta}. \quad (12)$$

Similarly, the average number of neighbors in SN_A of a node of SN_B, $\widetilde{\beta}_{B,A}$, satisfies

$$\widetilde{\beta}_{B,A} < \frac{\lambda_A P_B^\delta \mathbb{E}[G_{X^{B,A}}^\delta]}{\left(\sum_{i=1}^{N} \mu_i^{PT} P_i^\delta \mathbb{E}[G_{Y^{i,A}}^\delta]\right)(2^{R_B} - 1)^\delta}. \quad (13)$$

Note that $\widetilde{\beta}_{A,B}$ and $\widetilde{\beta}_{B,A}$ are different. $\widetilde{\beta}_{A,A}$ and $\widetilde{\beta}_{B,B}$ can be computed similarly. In the mean time, exact value and lower bound of the mean degree can be respectively derived by using Theorem III.2 and Theorem III.3.

In addition, the channel power gain of the interfering link from a transmitting node in $SN_u,\ u \in \{A, B\}$ to a PR in $PN_i,\ 1 \le i \le N$ is assumed to be drawn according to some distribution $f_{G_{Z^{u,i}}}$. An illustration is provided in Fig. 2(b). The active probability of an SU in SN_A (resp. SN_B) is denoted as p_A^a (resp. p_B^a). By using (9), p_A^a and p_B^a can be computed as

$$p_A^a = \exp\left(-\left(\sum_{i=1}^{N} \mu_i^{PR} \mathbb{E}[G_{Z^{A,i}}^\delta] \tau_i^{-\delta}\right) \pi P_A^\delta\right);$$
$$p_B^a = \exp\left(-\left(\sum_{i=1}^{N} \mu_i^{PR} \mathbb{E}[G_{Z^{B,i}}^\delta] \tau_i^{-\delta}\right) \pi P_B^\delta\right). \quad (14)$$

Now, we have the following theorem.

Theorem IV.1. *The percolation condition of the cooperative secondary network consisting of SN_A and SN_B is*

$$\begin{vmatrix} 1 - p_A^a \widetilde{\beta}_{A,A} & -p_A^a \widetilde{\beta}_{A,B} \\ -p_B^a \widetilde{\beta}_{B,A} & 1 - p_B^a \widetilde{\beta}_{B,B} \end{vmatrix} = 0, \quad (15)$$

$$\text{or,}\ (1 - p_A^a \widetilde{\beta}_{A,A})(1 - p_B^a \widetilde{\beta}_{B,B}) - p_A^a p_B^a \widetilde{\beta}_{A,B} \widetilde{\beta}_{B,A} = 0.$$

In addition, the mean component size of a cluster of connected and active SUs reachable from an SU of SN_A (resp. SN_B) is denoted as $\tilde{H}_0'^A(1)$ (resp. $\tilde{H}_0'^B(1)$), which satisfies

$$\begin{bmatrix}\tilde{H}_0'^A(1)\\ \tilde{H}_0'^B(1)\end{bmatrix} = \begin{bmatrix} p_A^a \\ p_B^a\end{bmatrix} + \begin{bmatrix} p_A^a\widetilde{\beta}_{A,A} & p_A^a\widetilde{\beta}_{A,B}\\ p_B^a\widetilde{\beta}_{B,A} & p_B^a\widetilde{\beta}_{B,B}\end{bmatrix} \begin{bmatrix}1-p_A^a\widetilde{\beta}_{A,A} & -p_A^a\widetilde{\beta}_{A,B}\\ -p_B^a\widetilde{\beta}_{B,A} & 1-p_B^a\widetilde{\beta}_{B,B}\end{bmatrix}^{-1} \begin{bmatrix}p_A^a\\ p_B^a\end{bmatrix}. \quad (16)$$

Proof: The proof is presented in Appendix E of [26]. ■

With cooperation, $\widetilde{\beta}_{A,B}$ and $\widetilde{\beta}_{B,A}$ are greater than zero. Let $C \triangleq \begin{bmatrix}1-p_A^a\widetilde{\beta}_{A,A} & -p_A^a\widetilde{\beta}_{A,B}\\ -p_B^a\widetilde{\beta}_{B,A} & 1-p_B^a\widetilde{\beta}_{B,B}\end{bmatrix}$, the mean component sizes $\tilde{H}_0'^A(1)$ and $\tilde{H}_0'^B(1)$ are proportional to $1/\det(C)$. When the first zero of $\det(C)$ is reached (i.e., equation (15)), the mean component size blows up indicating the formation of an infinite connected component in the cooperative secondary network. In the case without cooperation, $\widetilde{\beta}_{A,B}$ and $\widetilde{\beta}_{B,A}$ equal zero, recovering the percolation condition of a single secondary network SN_A (or SN_B). That is, (15) reduces to the percolation threshold $\widetilde{\beta}_{A,A} = 1/p_A^a$ (or $\widetilde{\beta}_{B,B} = 1/p_B^a$) as described in Section III-C.

Corollary IV.1. *By extending Theorem IV.1 to the case with cooperation among M heterogeneous secondary networks, the percolation condition becomes*

$$\begin{vmatrix} 1-p_1^a\widetilde{\beta}_{1,1} & -p_1^a\widetilde{\beta}_{1,2} & \cdots & -p_1^a\widetilde{\beta}_{1,M}\\ -p_2^a\widetilde{\beta}_{2,1} & 1-p_2^a\widetilde{\beta}_{2,2} & \cdots & -p_2^a\widetilde{\beta}_{2,M}\\ \vdots & \vdots & \ddots & \vdots\\ -p_M^a\widetilde{\beta}_{M,1} & -p_M^a\widetilde{\beta}_{M,2} & \cdots & 1-p_M^a\widetilde{\beta}_{M,M}\end{vmatrix} = 0, \quad (17)$$

where $\widetilde{\beta}_{i,j}$ is the average number of neighbors in secondary network j of an SU of secondary network i, and p_i^a is the active probability of an SU in secondary network i.

When all the off-diagonal entries are zero, (17) reduces to the percolation threshold of a single noncooperative secondary network.

A. Optimal power allocation

In the cooperative secondary network consisting of SN_A and SN_B, the effective total mean degree of an SU of SN_A (or SN_B) can be defined as the product of its active probability and its total mean degree in both SN_A and SN_B. For example, the effective total mean degree of an SU of SN_A is

$$p_A^a(\widetilde{\beta}_{A,A}+\widetilde{\beta}_{A,B}) = \exp\left(-\left(\sum_{i=1}^{N}\mu_i^{PR}\mathbb{E}[G_{Z^{A,i}}^{\delta}]\tau_i^{-\delta}\right)\pi P_A^{\delta}\right) \times \left(\frac{\lambda_A P_A^{\delta}\mathbb{E}[G_{X^{A,A}}^{\delta}]}{\left(\sum_{i=1}^{N}\mu_i^{PT}P_i^{\delta}\mathbb{E}[G_{Y^{i,A}}^{\delta}]\right)(2^{R_A}-1)^{\delta}} + \frac{\lambda_B P_A^{\delta}\mathbb{E}[G_{X^{A,B}}^{\delta}]}{\left(\sum_{i=1}^{N}\mu_i^{PT}P_i^{\delta}\mathbb{E}[G_{Y^{i,B}}^{\delta}]\right)(2^{R_A}-1)^{\delta}}\right). \quad (18)$$

Note that we use the upper bound on $\widetilde{\beta}_{A,A}$ and $\widetilde{\beta}_{A,B}$. When the transmit power of an SU of SN_A, P_A, decreases, its active probability increases; however, its total mean degree $\widetilde{\beta}_{A,A}+\widetilde{\beta}_{A,B}$ decreases. We maximize the effective total mean degree of an SU of SN_A with respect to P_A. After some calculations, the optimal transmit power is $P_A^* = \left(\pi\sum_{i=1}^{N}\mu_i^{PR}\mathbb{E}[G_{Z^{A,i}}^{\delta}]\tau_i^{-\delta}\right)^{-\delta^{-1}}$.

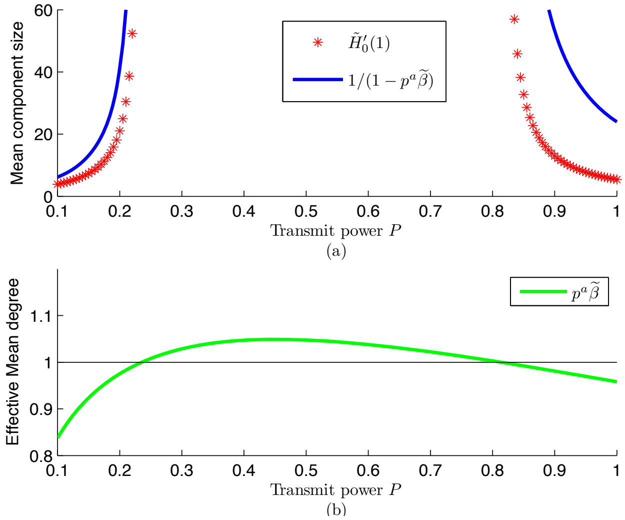

Fig. 3. Percolation of the secondary network SN_0 occurs (or the mean component size blows up) when the effective mean degree is greater than one, i.e., $p^a\widetilde{\beta} \geq 1$. The system parameters are set as $\lambda = 10^{-3}$, $R = 4$, $\alpha = 4$, $N = 1$, $\mu_1^{PT} = \mu_1^{PR} = 10^{-4}$, $P_1 = 0.15$, and $\tau_1 = 3.5\times 10^{-8}$. All links are Rayleigh faded with unit average power.

V. Numerical Results

Fig. 3 illustrates the site-percolation model in Section III-C. In Fig. 3(b), the relationship between the effective mean degree of an SU $p^a\widetilde{\beta}$ and its transmit power P is shown. When $p^a\widetilde{\beta} \geq 1$, the secondary network percolates and the mean component size $\tilde{H}_0'(1)$ blows up as shown in Fig. 3(a), indicating the formation of an infinite connected component in the secondary network. Note that when P is between 0.24 and 0.82, the secondary network percolates; while P is too large (i.e., the active probability p^a is extremely small) or too small (i.e., the mean degree $\widetilde{\beta}$ is extremely small) such that $p^a\widetilde{\beta} < 1$, the secondary network does not percolate.

Fig. 4 and Fig. 5 demonstrate the benefit of cooperation. In Fig. 4, the behavior of the cooperative secondary network consisting of SN_A and SN_B is studied. The transmit power of SN_A is varied from $P_A = 0.005$ to $P_A = 0.5$. When P_A increases, the changes of $p_A^a\widetilde{\beta}_{A,A}$ and $p_A^a\widetilde{\beta}_{A,B}$ are shown in Fig. 4(b). $p_B^a\widetilde{\beta}_{B,A}$ and $p_B^a\widetilde{\beta}_{B,B}$ do not change since they do not depend on P_A (note that P_B is fixed). With cooperation among SN_A and SN_B, the mean component size $\tilde{H}_0'^A(1)$ (resp. $\tilde{H}_0'^B(1)$) reachable from an SU of SN_A (resp. SN_B), which is proportional to $1/\det(C)$, blows up when the first zero of $\det(C)$ is reached, indicating the formation of an infinite connected component in the cooperative secondary network. In other words, percolation of the cooperative secondary network occurs when $\det(C) = (1-p_A^a\widetilde{\beta}_{A,A})(1-p_B^a\widetilde{\beta}_{B,B}) - p_A^a p_B^a\widetilde{\beta}_{A,B}\widetilde{\beta}_{B,A} \leq 0$. In Fig. 5, without cooperation, the mean component size of SN_A (resp. SN_B) never blows up since $p_A^a\widetilde{\beta}_{A,A} < 1$ (resp. $p_B^a\widetilde{\beta}_{B,B} < 1$). Note that $\widetilde{\beta}_{A,B} = \widetilde{\beta}_{B,A} = 0$

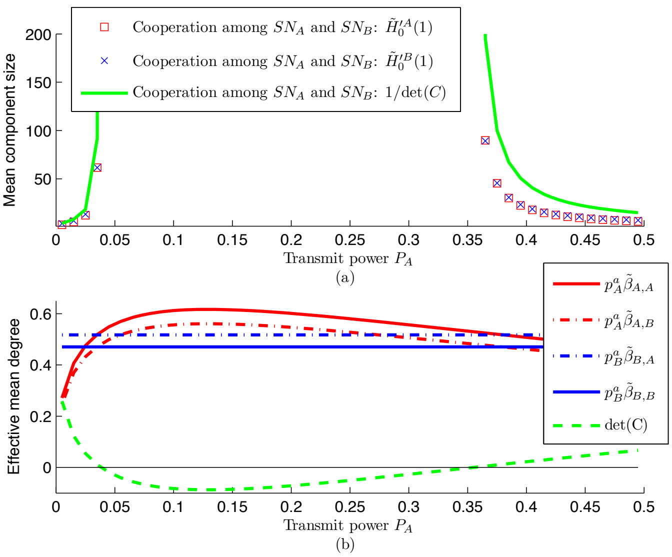

Fig. 4. With cooperation among SN_A and SN_B, percolation of the cooperative secondary network occurs (or the mean component size reachable from an SU of SN_A, $\tilde{H}_0'^A(1)$, or SN_B, $\tilde{H}_0'^B(1)$, blows up) when $\det(C) = (1 - p_A^a\widetilde{\beta}_{A,A})(1 - p_B^a\widetilde{\beta}_{B,B}) - p_A^a p_B^a \widetilde{\beta}_{A,B}\widetilde{\beta}_{B,A} \leq 0$. The system parameters are set as $\lambda_A = 1.1 \times 10^{-3}$, $R_A = 4$, $\lambda_B = 1 \times 10^{-3}$, $R_B = 3$, $P_B = 0.01$, $\alpha = 4$, $N = 1$, $\mu_1^{PT} = \mu_1^{PR} = 10^{-4}$, $P_1 = 0.15$, and $\tau_1 = 1 \times 10^{-8}$. P_A is varied from 0.005 to 0.5. All links are Rayleigh faded with unit average power.

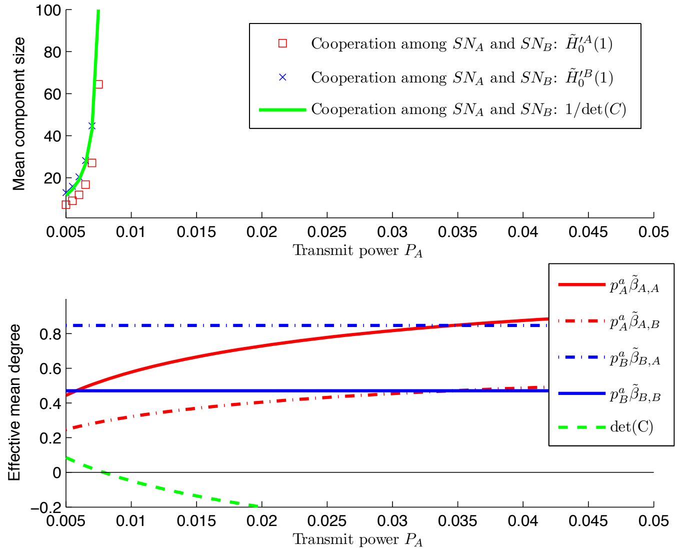

Fig. 6. With cooperation among SN_A and SN_B, percolation of the cooperative secondary network occurs when $\det(C) \leq 0$. The system parameters are set as $\lambda_A = 1.8 \times 10^{-3}$, $R_A = 4$, $\lambda_B = 1 \times 10^{-3}$, $R_B = 3$, $P_B = 0.01$, $\alpha = 4$, $N = 1$, $\mu_1^{PT} = \mu_1^{PR} = 10^{-4}$, $P_1 = 0.15$, and $\tau_1 = 1 \times 10^{-8}$. P_A is varied from 0.005 to 0.05. All links are Rayleigh faded with unit average power.

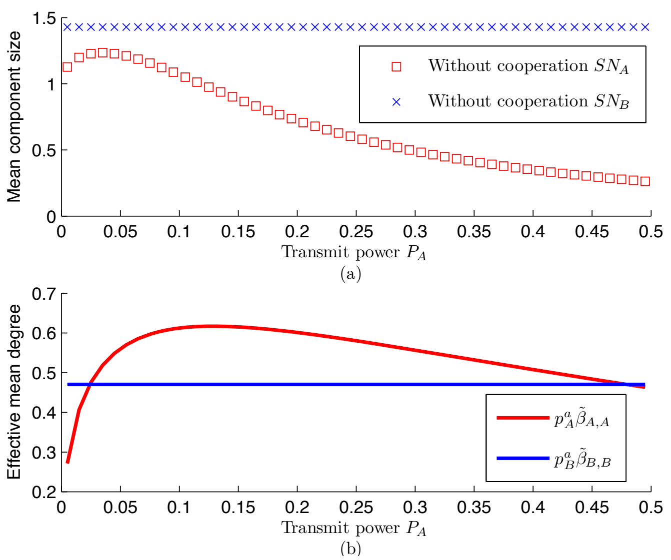

Fig. 5. Without cooperation, SN_A (resp. SN_B) does not percolate (or the mean component size does not blow up) since $p_A^a\widetilde{\beta}_{A,A} < 1$ (resp. $p_B^a\widetilde{\beta}_{B,B} < 1$). The system parameters are the same as in Fig. 4.

when there is no cooperation between SN_A and SN_B. This example demonstrates that percolation occurs only when both SN_A and SN_B cooperate with each other by having other network's nodes acting as relays.

In Fig. 6 and Fig. 7, we provide another example to illustrate the benefit of cooperation among SN_A and SN_B. The system parameters are the same as in Fig. 4 except that $\lambda_A = 1.8 \times 10^{-3}$. With cooperation among SN_A and SN_B, the mean component size $\tilde{H}_0'^A(1)$ (resp. $\tilde{H}_0'^B(1)$) reachable from an SU of SN_A (resp. SN_B) blows up when $P_A = 0.0075$ as shown in Fig. 6. In Fig. 7, without cooperation, the mean component size of SN_A blows up only when $P_A = 0.1$ (corresponding to $p_A^a\widetilde{\beta}_{A,A} = 1$); however, the mean component size of SN_B never blows up since $P_B = 0.01$ is fixed (corresponding to $p_B^a\widetilde{\beta}_{B,B} = 0.47 < 1$). This example demonstrates that percolation occurs much earlier (at lower P_A, $0.0075 < 0.1$) with cooperation among SN_A and SN_B, suggesting that SN_A can operate at lower transmit power to sustain the same level of connectivity. Power efficiency is therefore improved.

VI. Conclusion

We investigate the connectivity of cooperative secondary network from a percolation-based perspective by the following steps. First, the degree distribution of an SU is derived considering interference from multiple heterogeneous primary networks under general fading of desired signal and interfering signals. Second, the active probability of an SU is obtained considering interference temperature constraints at PRs. Third, the relationship between the degree distribution of an SU and the connectivity of the secondary network (with random node deactivation) in percolation sense is established by using the site-percolation model. Fourth, the above steps are extended to the analysis of connectivity of cooperative secondary network, in which each secondary network's node may have other secondary networks' nodes acting as relays. The benefit of cooperation among multiple secondary networks is analytically characterized in terms of the percolation threshold. Connectivity and energy efficiency of the CRN can be improved by the proposed cooperation framework.

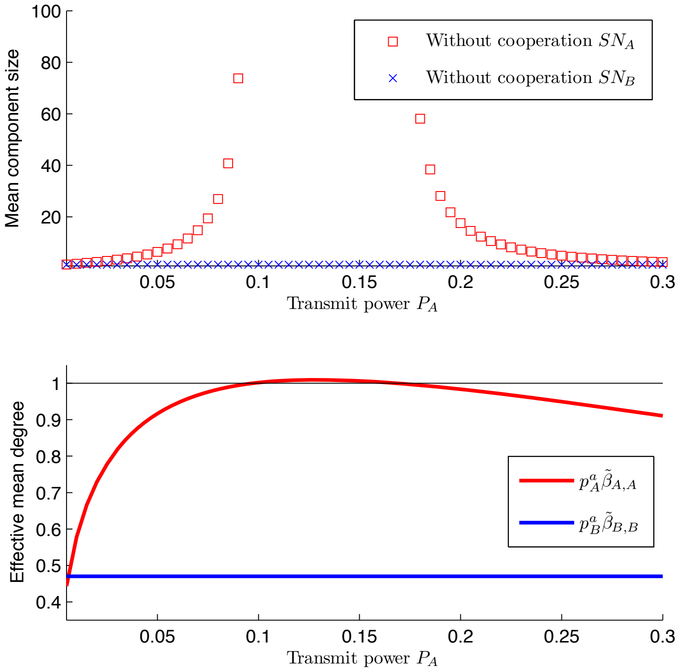

Fig. 7. Without cooperation, percolation of SN_A occurs when $P_A = 0.1$, and SN_B does not percolate. The system parameters are the same as in Fig. 6.

References

[1] I. Akyildiz, W. Lee, M. Vuran, and S. Mohanty, "NeXt generation/dynamic spectrum access/cognitive radio wireless networks: A survey," *Comput. Netw.*, vol. 50, no. 13, pp. 2127–2159, Sept. 2006.

[2] S. Haykin, "Cognitive radio: brain-empowered wireless communications," *IEEE J. Sel. Areas Commun.*, vol. 23, no. 2, pp. 201–220, Feb. 2005.

[3] A. Goldsmith, S. A. Jafar, I. Marić, and S. Srinivasa, "Breaking spectrum gridlock with cognitive radios: An information theoretic perspective," *Proc. IEEE*, vol. 97, no. 5, pp. 894–914, May 2009.

[4] Y. Xing, C. N. Mathur, M. Haleem, R. Chandramouli, and K. Subbalakshmi, "Dynamic spectrum access with qos and interference temperature constraints," *IEEE Trans. Mobile Comput.*, vol. 6, no. 4, pp. 423–433, Apr. 2007.

[5] P. Gupta and P. Kumar, "Critical power for asymptotic connectivity," in *Proc. IEEE CDC '98*, 1998.

[6] H. Zhang and J. Hou, "Asymptotic critical total power for k-connectivity of wireless networks," *IEEE/ACM Trans. Netw.*, vol. 16, no. 2, pp. 347–358, Apr. 2008.

[7] X. Ta, G. Mao, and B. Anderson, "On the giant component of wireless multihop networks in the presence of shadowing," *IEEE Trans. Veh. Technol.*, vol. 58, no. 9, pp. 5152–5163, Nov. 2009.

[8] P. Santi and D. Blough, "The critical transmitting range for connectivity in sparse wireless ad hoc networks," *IEEE Trans. Mobile Comput.*, vol. 2, no. 1, pp. 25–39, Jan. 2003.

[9] M. Franceschetti and R. Meester, *Random Networks for Communication: From Statistical Physics to Information Systems*. Cambridge University Press, 2008.

[10] D. Miorandi, E. Altman, and G. Alfano, "The impact of channel randomness on coverage and connectivity of ad hoc and sensor networks," *IEEE Trans. Wireless Commun.*, vol. 7, no. 3, pp. 1062–1072, Mar. 2008.

[11] M. Haenggi, "A geometric interpretation of fading in wireless networks: Theory and applications," *IEEE Trans. Inf. Theory*, vol. 54, no. 12, pp. 5500–5510, Dec. 2008.

[12] R. Hekmat and P. Mieghem, "Connectivity in wireless ad hoc networks with a log-normal radio model," *Mob. Netw. Appl.*, vol. 11, no. 3, pp. 351–360, June 2006.

[13] O. Dousse, F. Baccelli, and P. Thiran, "Impact of interferences on connectivity in ad hoc networks," *IEEE/ACM Trans. Netw.*, vol. 13, no. 2, pp. 425–436, Apr. 2005.

[14] Z. Kong and E. Yeh, "Connectivity and latency in large-scale wireless networks with unreliable links," in *Proc. IEEE INFOCOM '08*, Apr. 2008.

[15] D. Goeckel, B. Liu, D. Towsley, L. Wang, and C. Westphal, "Asymptotic connectivity properties of cooperative wireless ad hoc networks," *IEEE J. Sel. Areas Commun.*, vol. 27, no. 7, pp. 1226–1237, Sept. 2009.

[16] W. Ren, Q. Zhao, and A. Swami, "Connectivity of heterogeneous wireless networks," *IEEE Trans. Inf. Theory*, vol. 57, no. 7, pp. 4315–4332, July 2011.

[17] W. C. Ao, S.-M. Cheng, and K.-C. Chen, "Phase transition diagram for underlay heterogeneous cognitive radio networks," in *Proc. IEEE GLOBECOM '10*, Dec. 2010.

[18] P. Wang and I. Akyildiz, "Dynamic connectivity of cognitive radio ad-hoc networks with time-varying spectral activity," in *Proc. IEEE GLOBECOM '10*, Dec. 2010.

[19] R. Albert and A.-L. Barabási, "Statistical mechanics of complex networks," *Rev. Mod. Phys.*, vol. 74, no. 1, pp. 47–97, Jan. 2002.

[20] M. E. J. Newman, "The structure and function of complex networks," *SIAM Rev.*, pp. 167–256, 2003.

[21] D. S. Callaway, M. E. J. Newman, S. H. Strogatz, and D. J. Watts, "Network robustness and fragility: Percolation on random graphs," *Phys. Rev. Lett.*, vol. 85, no. 25, pp. 5468–5471, Dec. 2000.

[22] J. Kingman, *Poisson Processes*. Oxford University Press, 1993.

[23] M. E. J. Newman, S. H. Strogatz, and D. J. Watts, "Random graphs with arbitrary degree distributions and their applications," *Phys. Rev. E*, vol. 64, no. 2, p. 026118, July 2001.

[24] M. E. J. Newman, "Mixing patterns in networks," *Phys. Rev. E*, vol. 67, no. 2, p. 026126, Feb. 2003.

[25] M. Franceschetti, L. Booth, M. Cook, R. Meester, and J. Bruck, "Continuum percolation with unreliable and spread out connections," *J. of Statistical Physics*, vol. 118(3/4), pp. 721–734, Feb. 2005.

[26] W. C. Ao, S.-M. Cheng, and K.-C. Chen, "Connectivity of multiple cooperative cognitive radio ad hoc networks (extended version)," 2011. [Online]. Available: http://santos.ee.ntu.edu.tw/11jsac-long.pdf

[27] R. Ganti and M. Haenggi, "Spatial and temporal correlation of the interference in aloha ad hoc networks," *IEEE Commun. Lett.*, vol. 13, no. 9, pp. 631–633, Sept. 2009.

Weng Chon Ao was born in Macau. He received the B.S. degrees in both computer science and physics from National Taiwan University, Taiwan, in 2008, and the M.S. degree in communications engineering from National Taiwan University, Taiwan, in 2010. From 2010, he has been a research assistant with Intel-NTU lab, Taiwan. His research interests include stochastic modeling and control of communication networks.

Shin-Ming Cheng (S'05-M'07) received the B.S. and Ph.D. degrees in computer science and information engineering from National Taiwan University, Taipei, Taiwan, in 2000 and 2007, respectively. He joined the Graduate Institute of Communication Engineering, National Taiwan University, Taipei, Taiwan, as a postdoctoral research fellow in 2007. His research interests include wireless communications, network security, cognitive radio networks, and network science.

Kwang-Cheng Chen (M'89-SM'93-F'07) received his B.S. degree from National Taiwan University in 1983, and M.S. and Ph.D. degrees from the University of Maryland, College Park, in 1987 and 1989, all in electrical engineering. From 1987 to 1998 he was with SSE, COMSAT, the IBM Thomas J. Watson Research Center, and National Tsing Hua University, Hsinchu, Taiwan, working on mobile communications and networks. He is a Distinguished Professor and Director of the Graduate Institute of Communication Engineering and the Communication Research Center, National Taiwan University. He has received numerous awards and honors, including co-authoring 3 IEEE papers to receive ISI Classic Citation Award, the IEEE ICC 2010 Best Paper Award, and IEEE GLOBECOM 2010 GOLD Best Paper. His research interests include wireless communications and network science.